Synthesis of nanostructured ThO 2 pellets

Emanuele de Bona, Olaf Walter, Heike Störmer, Thierry Wiss, Gianguido Baldinozzi, Marco Cologna, Karin Popa

Received: 7 January 2019 | Accepted: 2 February 2019

DOI: 10.1111/jace.16375

RAPID COMMUNICATION

Journal of the American Ceramic Society

Synthesis of nanostructured ThO_2 pellets

Emanuele De Bona[1,2] | **Olaf Walter**[1] | **Heike Störmer**[3] | **Thierry Wiss**[1] | **Gianguido Baldinozzi**[2] | **Marco Cologna**[1] | **Karin Popa**[1]

[1]European Commission, Joint Research Centre, Nuclear Safety and Security Directorate, Karlsruhe, Germany

[2]Laboratoire Structures, Propriétés et Modélisation des Solides, CNRS, CentraleSupélec, Université Paris-Saclay, Gif-sur-Yvette, France

[3]Laboratory for Electron Microscopy, Karlsruhe Institute of Technology (KIT), Karlsruhe, Germany

Correspondence
Emanuele De Bona, European Commission, Joint Research Centre, Nuclear Safety and Security Directorate, Karlsruhe, Germany.
Email: emanuele.de-bona@ec.europa.eu

Abstract

We present here for the first time the production of 3- to 5-nm–sized thoria nanopowders by decomposition of Th-hydroxide under hot compressed water and their consolidation by high-pressure spark plasma sintering into dense nanostructured ThO_2 with grain size of 50 nm.

KEYWORDS

decomposition of hydroxides under hot compressed water, high burn-up structure (HBS), nanostructured ceramics, spark plasma sintering, thorium oxide

1 | INTRODUCTION

The bulk properties of ceramic materials are largely dependent on the crystallite size, and the role of the grain boundaries plays an increasing role when extending into the nanodomain range (<100 nm). The sintering of bulk ceramic materials with high relative mass density (>90%-95%) maintaining a nanometric grain size is particularly challenging: it requires the synthesis of suitable nanopowders and their sintering into a dense material. The densification is, however, always associated with grain growth, so that the initial nanostructure of the starting powders is often lost.[1] This is even more challenging for actinides oxides, due to the additional safety and radiological issues related to their manipulation. As a result, little is known concerning the properties of nanostructured actinides oxides.

Nanocrystalline ceramics are believed to be more resistant to radiation damage, because of grain boundaries which can act as sinks for radiation-induced defects.[2] This is particularly of interest for ThO_2 and UO_2 due to their use in nuclear applications. The rim of nuclear fuels at extended burn-up transforms into a porous and nanograined region, commonly called high burn-up structure (HBS),[3] addressing that the properties of nanostructured actinides oxides is not only a fundamental problem, but is also of technological importance.

Dense ThO_2 pellets were recently obtained starting from nanocrystalline ThO_2 powders synthesized either by the citrate gel-combustion method and two-step sintering with a first target temperature of 1600°C,[4] or from oxalate precipitation and one-step sintering at 1750°C for 8 hours.[5] Electric field–assisted techniques, such as SPS[6] and flash sintering,[7] were used in an attempt to limit grain growth of ThO_2 powder from oxalate precipitation: submicrometer-grained dense ThO_2 was obtained by SPS at 1600°C,[8] while flash sintering under an electric field of 500 V/cm yielded 250-nm grained pellets with a relative density higher than 0.95.[9] In order to further limit grain growth during sintering, the maximum temperature needs to be minimized. The onset of the sintering shifts to lower temperatures as the applied pressure increases[8,10]; however, the strength of graphite allows applying up to ~100 MPa. Nanocrystalline ceramic oxides (well below 100 nm grain size) can be obtained with the high-pressure (HP)-SPS method, by using special WC or SiC inserts instead of lower strength graphite.[11,12] In this way, nanocrystalline

UO_2 disks (average grain size in the order of 50 nm) were recently achieved.[13,14]

Advanced methods for the production of nanocrystalline oxide materials were developed during the last years. Very recently, we have reported the decomposition of oxalates under hot compressed water[15–17] to obtain highly sinterable actinide oxides nanopowders. We have extended this method toward decomposition of other substances. We present here the first results of the production of highly sinteractive nano-ThO_2 powder by mild decomposition of Th-hydroxide under hot compressed water at very low temperature (down to 200°C). Dense and nanograined ThO_2 monoliths were obtained for the first time by sintering the powders using HP-SPS at 915°C.

2 | MATERIALS AND METHODS

2.1 | Powder synthesis and material processing

The thoria nanopowders used in this study were obtained by decomposition of thorium hydroxide under hot compressed water. $Th(OH)_4$ powder produced by direct precipitation of a thorium solution (1.9 M in 8 M HNO_3) with ammonia was placed in a 25-mL Teflon-lined hydrothermal synthesis autoclave reactor with 10 mL distilled water and reacted for 22 hours at 200-320°C and autogenic pressure under continuous stirring. The final product consisted of pure nanocrystalline thoria which could be easily separated from the solution; in order to remove the water that is potentially absorbed at the surface, the nanocrystals were repeatedly washed with ethanol and acetone and then dried in air.

The powders were compacted in a small-sized SPS (FCT Systeme GmbH) integrated in a glovebox for the handling of radioactive materials.[18–20] Sintering was performed under vacuum with 50/5 ms current/pause intervals. The regular setup consists of graphite punches and die with an inner diameter of 6 mm, filled with 250-300 mg of powder to achieve sintered disks with height of about 1 mm, and prepressed at 0.5 kN (17.7 MPa).The sintering treatment consisted of the following steps: (a) heating to 250°C at 100°C/min under 0.5 kN (17.7 MPa pressure); (b) application of 2 kN (70 MPa) at constant temperature; (c) heating to 1050, 1200 or 1600°C at 200°C/min; (d) 10 minutes dwell at maximum temperature; and (e) cooling to room temperature at 200°C/min maintaining a force of 2 kN (70 MPa).

The HP SPS consisted of SiC die and punches (4 and 12 mm inner and outer diameter, respectively) placed inside a graphite setup raising the applicable force from 2-3 kN (70-100 MPa in a 6 mm die) to 6.3 kN (500 MPa in a 4 mm die). In this second process, 150 mg of powder were filled in the die and prepressed at 0.5 kN (39.8 MPa), before applying the following treatment: (a) heating to 250°C at 100°C/min with an applied force of 0.5 kN (39.8 MPa); (b) raising the force to 6.3 kN (500 MPa) in 30 seconds with three load/unload cycles to break powder agglomerates; (c) heating to the maximum temperature (915°C) at 200°C/min; and (d) without any dwell time, cooling to room temperature at 200°C/min with 6.3 kN applied force.

The densification can be followed by monitoring the displacement of the piston. A positive displacement rate of the upper piston indicates shrinkage. The plots are reported without baseline correction for thermal expansion and mechanical load.

In regular SPS, the temperature of the sample is measured through a thermocouple inserted in the lower piston ending 2 mm below the surface in contact with the powder. With the HP setup, the insertion of the additional SiC components results in an increased distance between powder and thermocouple, and thus, a less accurate measurement of the actual sample temperature (which does not hinder the reproducibility of the process).

2.2 | Physicochemical characterization

XRD analyses were performed on a Rigaku Miniflex 600 X-ray diffractometer (equipped with advanced Hy-Pix 400MF

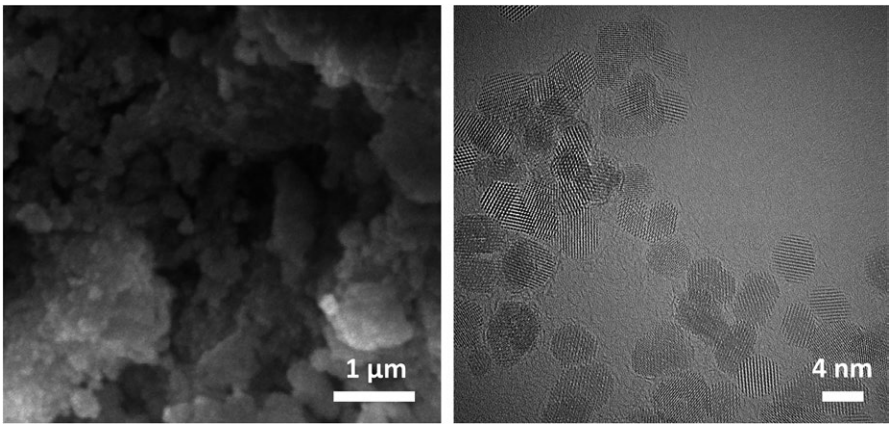

FIGURE 1 Morphology of the ThO_2 agglomerated powder (SEM picture on the left) and TEM image of the primary particles (right)

TABLE 1 Properties of ThO_2 powder by hydrothermal decomposition of thorium hydroxide under hot compressed water

Reaction temperature, °C	*a* lattice parameter, Å	Particle size, nm	
		From XRD	From TEM
200	5.605 (2)	2.9 (1)	3.3 (5)
230	5.607 (2)	3.9 (2)	4.1 (7)
320	5.608 (1)	4.7 (4)	5.0 (10)

2D HPAD detector, high-flux 600 W X-ray source, operating at 40 kV and 15 mA). The average crystallite size was calculated with the Williamson-Hall approach[21] after correction for instrumental broadening and compared with the particle size measured from TEM and SEM images.

Scanning electron microscopy (SEM) images were recorded using a Tescan Vega TS5130LSH operated at 20 KeV for powders and a dual-beam SEM by FEI™ operated at 30 KeV for disks. The grain size was estimated on the fracture surfaces micrographs with the intercept method without applying a correction factor. Transmission electron microscopy (TEM) on powders was performed using an aberration (image) corrected FEI™ Titan 80-300 operated at 300 kV providing a nominal information limit of 0.8 Å in TEM mode and a resolution of 1.4 Å in scanning transmission electron microscopy (STEM) mode. TEM images have been recorded using a Gatan US1000 slowscan CCD camera, and STEM images have been recorded using a Fischione high-angle annular dark-field (HAADF) detector with a camera length of 195 mm. The samples for analysis have been prepared on carbon-coated copper grids by drop coating with a suspension of the nanoparticles in ultrapure water. TEM on the sintered material was performed using a TecnaiG2 (FEI™) 200 kV equipped with Gatan™ Tridiem GIF camera, and a high-angle annular dark-field (HAADF) detector for STEM imaging.

3 | RESULTS AND DISCUSSIONS

The decomposition of actinide hydroxides under hot compressed water is an enhanced method (derived from the

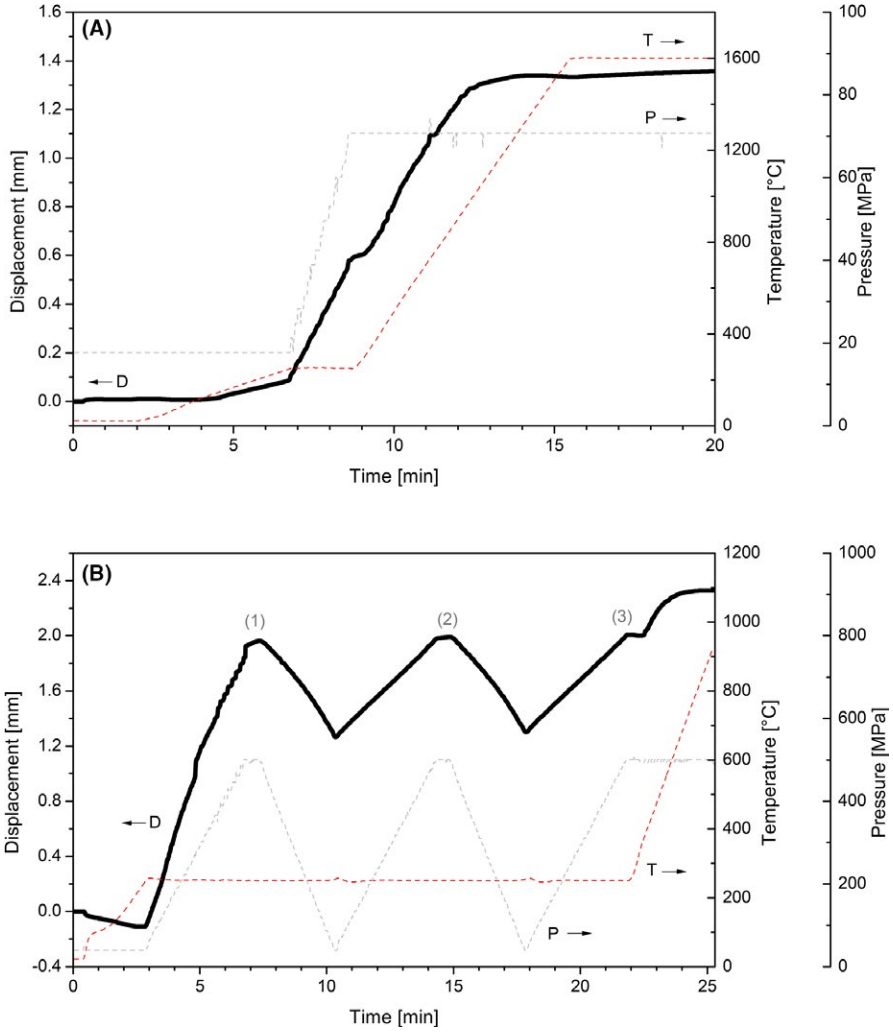

FIGURE 2 A and B, Sintering behavior of nano-ThO2 powder in SPS with 70 MPa (A) and 500 MPa (B) applied load [Colour figure can be viewed at wileyonlinelibrary.com]

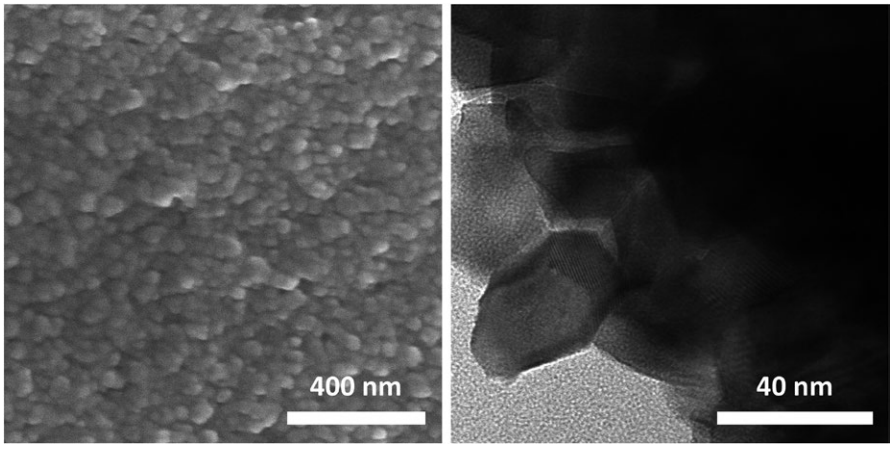

FIGURE 3 Nanograined ThO_2 disk made by HP-SPS: SEM of a fracture surface (left) and TEM (right)

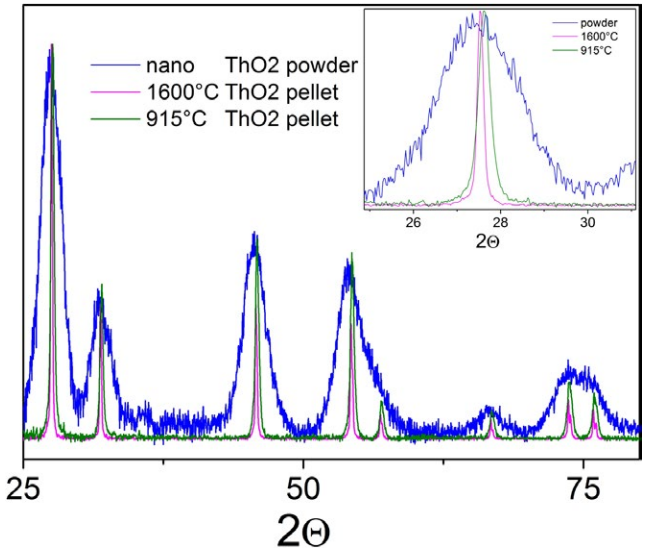

FIGURE 4 XRD patterns of ThO_2 nanopowders and sintered disks. The crystallite size is inversely proportional to the peak breadth [Colour figure can be viewed at wileyonlinelibrary.com]

actinide oxalate hydrothermal decomposition process) which can be successfully applied for the production of nano-sized actinide oxide powders. The ThO_2 powders obtained through this method consist of soft agglomerates (Figure 1) which were easily dispersed in water or ethanol. For SPS studies, the nanopowders obtained at 230°C were used, with a primary particle size of about 4 nm (Table 1).

Sintering in a conventional SPS graphite assembly was conducted at three different temperatures (1050, 1200, and 1600°C). Only the highest temperature allowed reaching high density; however, residual porosity was evident from the microstructural analysis and significant grain growth could not be avoided because of the high temperature. The microstructure was also not homogeneous: area with submicrometer grains (approximately 0.5 μm) were found close to areas with larger grains (1-2 μm). Residual porosity and inhomogeneous microstructure are an indication of the presence of agglomerates and non-optimal powder packing. The sintering curve is reported in Figure 2A. The maximal pressure was applied only from the temperature of 250°C to allow for degassing. Until such temperature, the system was heated with the minimum applied force allowed by the device (0.5 kN). The piston displacement observed already from a temperature of around 100°C in Figure 2 is likely an indication of the beginning of removal of adsorbed water. After the application of maximum processing pressure (70.7 MPa) at 250°C, the displacement continues during the heating ramp to 1600°C and also during the 10 minutes dwell.

The sintering curves during HP-SPS are given in Figure 2B. The application of a cyclic load at 250°C has the effect of a net gain in the piston displacement of 28 μm in step 2 and 18 μm in step 3 (corresponding to approximately 0.8 and 0.5 relative density, respectively, to reach the green relative density of 58% at step 3). This indicates the breaking of agglomerates or particle rearrangement under pressure and degassing. Densification continues at high rate until the maximum set temperature of 915°C. The geometrical measurement of the final density is subjected to large errors because of the irregular shape; the sample was also too small for accurate Archimedes density measurements. However, as seen in Figure 3, microstructural analysis reveals the almost complete absence of porosity (SEM) and grains with polygonal shape (TEM) typical of densified material. Notably, the grain size has remained extremely fine.

Figure 4 illustrates the comparison among the XRD patterns of the starting ThO_2 nanopowder and two sintered disks (1600 and 915°C). The low-temperature disk shows peaks that are significantly broader than the high-temperature ones, testifying once more the reduced grain coarsening during the process. The final grain size is in the order of 50 nm, as estimated from the line intercept method and from the XRD peak broadening.

4 | CONCLUSIONS

ThO_2 nanopowders with particle sizes in the range of 4 nm were produced by hydrothermal decomposition of Th-hydroxide under hot compressed water. Densification of such powders under typical SPS conditions (pressures up to 70 MPa) was possible at 1600°C, although significant grain growth occurred. Increasing the applied pressure at 500 MPa by using SiC dies allowed densification at 915°C, limiting the grain growth. For the first time, a route toward the synthesis of dense nanograined ThO_2 disks with a grain size of ~50 nm is reported. Such model material will allow the study of the effect of the grain boundaries on the macro- and microscopic properties of ThO_2.

ACKNOWLEDGMENTS

The technical support provided by Michael Holzhäuser, Oliver Dieste Blanco, Markus Ernstberger, and Antonio Bulgheroni is highly appreciated. This work contributes to the Joint Programme on Nuclear Materials (JPNM) of the European Energy Research Alliance (EERA).

ORCID

Emanuele De Bona https://orcid.org/0000-0001-5133-5108

Gianguido Baldinozzi https://orcid.org/0000-0002-6909-0716

REFERENCES

1. Maglia F, Tredici IG, Anselmi-Tamburini U. Densification and properties of bulk nanocrystalline functional ceramics with grain size below 50 nm. J Eur Ceram Soc. 2013;33(6):1045–66.
2. Dey S, Drazin JW, Wang Y, Valdez JA, Holesinger TG, Uberuaga BP, et al. Radiation tolerance of nanocrystalline ceramics: Insights from yttria stabilized zirconia. Sci Rep. 2015;5:7746.
3. Matzke H, Kinoshita M. Polygonization and high burnup structure in nuclear fuels. J Nucl Mater. 1997;247:108–15.
4. Sanjay Kumar D, Ananthasivan K, Venkata Krishnan R, Amirthapandian S, Dasgupta A. Studies on the synthesis of nanocrystalline Y2O3 and ThO2 through volume combustion and their sintering. J Nucl Mater. 2016;479:585–92.
5. Wangle T, Tyrpekl V, Cagno S, Delloye T, Larcher O, Cardinaels T, et al. The effect of precipitation and calcination parameters on oxalate derived ThO_2 pellets. J Nucl Mater. 2017;495:128–37.
6. Inoue K. Apparatus for electrically sintering discrete bodies. US Patent 1966, 3,250,892.
7. Raj R, Cologna M, Prette ALG, Sglavo VM, Francis J. Methods of flash sintering. U.S. Patent. 2015, 8,940,220.
8. Tyrpekl V, Cologna M, Robba D, Somers J. Sintering behaviour of nanocrystalline ThO_2 powder using spark plasma sintering. J Eur Ceram Soc. 2016;36:767–72.
9. Straka W, Amoah S, Schwartz J. Densification of thoria through flash sintering. MRS Commun. 2017;7(3):677–82.
10. Munir ZA, Anselmi-Tamburini U, Ohyanagi M. The effect of electric field and pressure on the synthesis and consolidation of materials: A review of the spark plasma sintering method. J Mat Sci. 2006;41:763–77.
11. Anselmi-Tamburini U, Garay JE, Munir ZA. Fast low-temperature consolidation of bulk nanometric ceramic materials. Scr Mater. 2006;54(5):823–8.
12. Grasso S, Kim BN, Hu C, Maizza G, Sakka Y. Highly transparent pure alumina fabricated by high-pressure spark plasma sintering. J Am Ceram Soc. 2010;93(9):2460–2.
13. Tyrpekl V, Cologna M, Vigier JF, Cambriani A, De Weerd W, Somers J. Preparation of bulk-nanostructured UO_2 pellets using high-pressure spark plasma sintering for LWR fuel safety assessment. J Am Ceram Soc. 2017;100:1269–74.
14. Yao T, Scott SM, Xin G, Gong B, Lian J. Dense nanocrystalline UO_{2+x} fuel pellets synthesized by high pressure spark plasma sintering. J Am Ceram Soc. 2018;101:1105–15.
15. Walter O, Popa K, Blanco OD. Hydrothermal decomposition of actinide(IV) oxalates: A new aqueous route towards reactive actinide oxide nanocrystals. Open Chem. 2016;14:170–4.
16. Balice L, Bouëxière D, Cologna M, Cambriani A, Vigier J-F, De Bona E, et al. Nano and micro $U_{1-x}Th_xO_2$ solid solutions: From powders to pellets. J Nucl Mater. 2018;498:307–13.
17. Popa K, Walter O, Blanco OD, Guiot A, Bouëxière D, Colle JY, et al. A low-temperature synthesis method for AnO_2 nanocrystals (An = Th, U, Np, and Pu) and associate solid solutions. CrystEngComm. 2018;20:6414–22.
18. Tyrpekl V, Berkmann C, Holzhäuser M, Köpp F, Cologna M, Wangle T, et al. Implementation of a spark plasma sintering facility in a hermetic glovebox for compaction of toxic, radiotoxic, and air sensitive materials. Rev Sci Instrum. 2015;86:023904.
19. Tyrpekl V, Holzhäuser M, Hein H, Vigier JF, Somers J, Svora P. Synthesis of dense yttrium-stabilised hafnia pellets for nuclear applications by spark plasma sintering. J Nucl Mater. 2014;454:398–404.
20. Wangle T, Tyrpekl V, Cologna M, Somers J. Simulated UO_2 fuel containing CsI by spark plasma sintering. J Nucl Mater. 2015;466:150–3.
21. Williamson GK, Hall WH. X-ray line broadening from filed aluminium and wolfram. Acta Metall. 1953;1(1):22–31.

How to cite this article: De Bona E, Walter O, Störmer H, et al. Synthesis of nanostructured ThO_2 pellets. *J Am Ceram Soc*. 2019;102:3814–3818. https://doi.org/10.1111/jace.16375